FULL PAPER

Dalton
www.rsc.org/dalton

New powerful reagents based on dihalogen/*N*,*N*′-dimethylperhydrodiazepine-2,3-dithione adducts for gold dissolution: the IBr case †

Lorenzo Cau,[a] Paola Deplano,[a] Luciano Marchiò,[b] Maria Laura Mercuri,*[a] Luca Pilia,[a] Angela Serpe[a] and Emanuele F. Trogu[a]

[a] *Dipartimento di Chimica Inorganica e Analitica, Università di Cagliari, S.S. 554 – bivio per Sestu, I-09124 Monserrato (CA), Italy. E-mail: mercuri@unica.it*

[b] *Dipartimento di Chimica Generale ed Inorganica, Chimica Analitica, Chimica Fisica, Università di Parma, Parco delle Scienze 17A, I-43100 Parma, Italy*

Received 21st October 2002, Accepted 13th December 2002
First published as an Advance Article on the web 23rd April 2003

The synthesis, X-ray structure [monoclinic, $P2_1/n$, $a = 12.1690(1)$, $b = 7.8360(1)$, $c = 14.4250(1)$ Å, $\beta = 113.808(2)°$], spectroscopic and electrochemical characterization of a new powerful reagent based on the iodine monobromide adduct of the *N*,*N*′-dimethylperhydrodiazepine-2,3-dithione (Me_2dazdt) ligand, able to oxidize gold metal in a one-step reaction under mild conditions, is reported. The gold metal dissolution has been performed on gold powder, wires and Au/Ti thin layers. The oxidation product has been isolated and structurally characterised as $[Au(Me_2dazdt)Br_2]IBr_2$ [monoclinic, $C2/c$, $a = 26.523(8)$, $b = 10.191(6)$, $c = 14.549(7)$ Å, $\beta = 111.57(2)°$]. The metal is essentially within a square planar geometry, Me_2dazdt acts as an *S*,*S* chelating ligand and two bromide ligands complete the geometry around the metal. The IBr_2^- counteranion is essentially linear and shows I–Br bond lengths slightly asymmetric [Br(4)–I(1) 2.742(3), Br(3)–I(1) 2.682(2) Å]. A comparison with the gold removal from Si/SiO_2/Au/Ti thin layers of comparable thickness to that found in microelectronic devices, by using THF solutions of IBr and I_2 adducts of the Me_2dazdt donor, as well as the currently used I_2/I^- aqueous solutions, shows that these dihalogens-adducts produce a quantitative gold removal in shorter times and leaving the underlying layer perfectly clean, and are thus highly desirable as new etching agents in the gold-based technology of semiconductor devices.

Introduction

The recovery of noble-metals is assuming increasing environmental and economic relevance because of waste accumulation and the simultaneous decrease of raw materials due to their extensive usage in novel technologies (catalytic converters, electronic devices).[1] Among them gold removal is of special interest within the failure analysis of microelectronic devices.[2] Currently used methods do not give satisfactory results for the dissolution of the metals which constitute the "platinum metal-group": the safer ones often show low effectiveness (iodide/iodine mixtures), the more effective are often unattractive (*e.g.* boiling aqua-regia, mercury and cyanide are still in use in the mine industry) and their use will be limited in the near future as a result of EC safety regulations.[3]

Much effort has been devoted to the search for effective reagents which are safer for the operators, non-polluting and easy to handle.[4,5] A simple, non-polluting and potentially revolutionary method is based on the use of diiodine adducts with appropriate donors, where complexing and oxidizing properties coexist in the same molecule. This method, pioneered by the McAuliffe group[6] using phosphines and arsines as donors, works well in gold metal powder activation (the $[AuI_3(Me_3As)]$ and $[AuI_3(Me_3P)_2]$ complexes have been obtained and fully characterized). However, diiodine adducts with phosphine and arsine donors are unsuitable for practical applications since they require strictly anhydrous, anaerobic conditions, long reaction times and due to the toxicity of the donors themselves! Other dihalogen adducts such as the I_2/I^- system in CH_3CN have been successfully used by Nakao and Sone[7] to dissolve/deposit noble-metals on heating/cooling the resulting solution.

We have extensively studied the diiodine-adducts with S-donors and equilibria, structural, spectroscopic (in particular by Raman spectroscopy) and theoretical studies have been performed to better understand the nature of the diiodine/donor bonding.[8–10] On this basis, cyclic dithio-oxamides, molecules bearing two vicinal thioamide groups, have been selected as donors to prepare a new class of diiodine adducts. Our working hypothesis was that the proper choice of polyfunctional donors, which can favour the preferred geometry required by the metal (in this case the square-planar geometry) and give chelation, should add a favorable condition to the spontaneity and selectivity of the oxidation reaction. The results obtained, for instance using the bis-diiodine adduct of *N*,*N*′-dimethylperhydrodiazepine-2,3-dithione (Me_2dazdt = **1**),[11] a cyclic dithio-oxamide with a heptatomic ring, which is inert towards air/moisture and does not show cytotoxicity, show that this reagent is capable of oxidizing gold in a one-step reaction, under mild conditions and in a short time to produce the square-planar $[Au(Me_2dazdt)I_2]I_3$ complex.[12] It is not active towards Pt either at room temperature or in refluxing THF and CH_3CN. The corresponding reaction of diiodine with *N*,*N*′-dimethylpiperazine-2,3-dithione (Me_2pipdt = **2**) (the cyclic dithio-oxamide with a hexatomic ring), produces a triiodide of the monocation of the donor, the $[Me_2pipdt]I_3$ salt. By reacting this salt with metallic platinum in a stoichiometric ratio, the $[Pt(Me_2pipdt)_2](I_3)_2$ complex is obtained in high yield.[13]

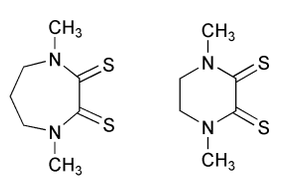

1 **2**

† Based on the presentation given at Dalton Discussion No. 5, 10–12th April 2003, Noordwijkerhout, The Netherlands.

Electronic supplementary information (ESI) available: molecular drawing of the dimeric species $[\mathbf{1}\cdot IBr]_2$. See http://www.rsc.org/suppdata/dt/b2/b210281a/

DOI: 10.1039/b210281a

Table 1 Selected bond lengths (Å) and angles (°) for Me_2dazdt·IBr

C(1)–N(1)	1.321(5)	C(4)–C(5)	1.525(6)
C(1)–C(2)	1.498(5)	C(5)–N(1)	1.490(5)
C(1)–S(1)	1.651(4)	C(6)–N(1)	1.467(5)
C(2)–N(2)	1.310(4)	N(2)–C(7)	1.460(5)
C(2)–S(2)	1.696(4)	S(2)–I	2.575(1)
C(3)–N(2)	1.486(5)	Br–I	2.7520(6)
C(3)–C(4)	1.511(6)		
N(1)–C(1)–C(2)	116.1(3)	C(1)–N(1)–C(6)	120.3(4)
N(1)–C(1)–S(1)	127.7(3)	C(1)–N(1)–C(5)	119.8(3)
C(2)–C(1)–S(1)	116.0(3)	C(6)–N(1)–C(5)	119.0(4)
N(2)–C(2)–C(1)	116.2(3)	C(2)–N(2)–C(7)	123.0(3)
N(2)–C(2)–S(2)	121.3(3)	C(2)–N(2)–C(3)	118.9(3)
C(1)–C(2)–S(2)	122.5(3)	C(7)–N(2)–C(3)	118.0(3)
N(2)–C(3)–C(4)	110.8(3)	C(2)–S(2)–I	106.43(14)
C(3)–C(4)–C(5)	111.9(3)	S(2)–I–Br	175.91(3)
N(1)–C(5)–C(4)	111.2(3)		

On the basis of these promising results, we are now addressing our efforts to check for the feasibility of these adducts for practical applications. Among these, selective gold removal from the Ti/Pt/Au triple metal system in GaAs-based devices is of special interest for the failure analysis. A (Me_2dazdt)·$2I_2$ adduct's acetone solution has been shown to be capable of etching selectively the gold layer without damaging the underlying layers.[14]

As a progression of these studies we are investigating the corresponding reactions of the adducts of these cyclic dithiooxammides on varying the dihalogen (I_2, IBr, ICl). By changing the halogens we expect to further tune the oxidation power of the adducts.

In this paper we report the case of the Me_2dazdt-iodine monobromide adduct.

Results and discussion

By reacting Me_2dazdt (**1**) with IBr (1 : 2 molar ratio) in $CHCl_3$ solution yellow–orange microcrystals, that can be formulated as Me_2dazdt·2IBr on the basis of analytical results, were obtained by slow evaporation of the solvent at room temperature. After recrystallization from CH_3CN well-shaped orange crystals of Me_2dazdt·IBr were collected and characterized by X-ray analysis. The molecular structure of this adduct is shown in Fig. 1, crystallographic data are reported in Table 3 (see Experimental), with selected bond lengths and angles in Table 1.

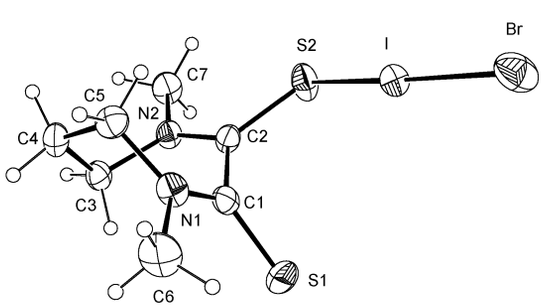

Fig. 1 Molecular structure of Me_2dazdt·IBr. Thermal ellipsoids are drawn at the 30% probability level.

The seven membered ring of the ligand adopts a "twist" conformation with a pseudo two-fold axis passing through the middle point of the C(1)–C(2) bond and the C(3) atom and its structural data are quite similar to those observed in the corresponding diiodine adduct Me_2dazdt·$2I_2$[11] and in the complexes [Au(Me_2dazdt)I_2]I_3,[12] [Ni(Me_2dazdt)$_3$](BF_4)$_2$[15] and [Ni(Me_2dazdt)(mnt)].[15] The molecule is chiral but both enantiomers are present in the structure (space group $P2_1/n$). The electron delocalization is limited to the S(1)–C(1)–N(1) and S(2)–C(2)–N(2) fragments; these thioamide groups are essentially planar but are skewed with respect to each other limiting a possible conjugation of the two systems; in fact the torsion angle τ[N(1)–C(1)–C(2)–N(2)] is −67.8(5)°. A very weak contact of the type S ··· I [3.960(2) Å] is present involving the S(2) and I atoms of two adjacent molecules giving rise to a dimeric unit in the solid state (see ESI).† The I–Br vector, which is quasi-collinear with the S(2)–I one [S(2)–I–Br = 175.91(3)°], is elongated with respect to that in the free IBr molecule [2.7520(6) *vs.* 2.521(4) Å][16] as a consequence of the mixing of the donor orbital with the σ* antibonding orbital of IBr. The S(2)–I bond distance [2.575(1) Å] is significantly shorter than that found in the corresponding I_2-adduct (2.786 Å) and in related S-donors I_2 adducts [mean 2.72(3) Å],[10,17] in accordance with the more acid character of IBr with respect to I_2. It is noteworthy that only few adducts of S-donors with IBr have been reported in the literature and characterized by X-ray diffraction studies.[18] While the S–I and IBr distances suggest that Me_2dazdt·IBr may be taken as a strong adduct of type **2** (three-body S–I–Br system) according to the classification that we have proposed for D–I_2 adducts,[9] a theoretical study is required to deeper understand the nature of the bond in this adduct. A Raman broad peak centered at 162 cm^{-1} with a shoulder at approximately 145 cm^{-1} may be tentatively assigned to the ν_3 and ν_1 stretching vibrations of the S–I–Br group if it may be taken as an asymmetric linear triatomic system where three Raman active vibrations [the symmetric (ν_1), the antisymmetric (ν_3) stretches and the (ν_2) bending] are expected.[19] Further studies, including far IR experiments, are required to support this tentative assignment.

The reaction of Me_2dazdt·2IBr with gold, in a 2 : 1 molar ratio, performed using the metal as a powder (50–5 mesh), wires (0.25 mm diameter) and thin films (Au/Ti, 200 nm/15 nm thick), is summarized in Scheme 1.

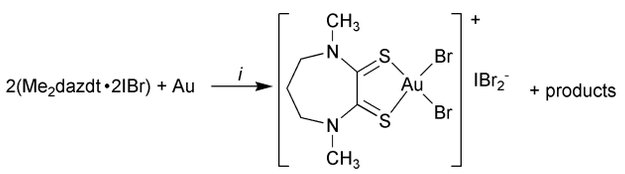

Scheme 1 (i) THF, room temperature, 30 min to dissolve 22 mg of gold.

The gold dissolution is achieved under mild conditions (room temperature). The reaction seems unaffected by the presence of air and/or moisture, proceeding similarly under unaerobic conditions or without any protection from the air and/or moisture. The obtained product [Au(Me_2dazdt)Br_2]IBr_2 has been structurally characterised. The molecular structure of the [Au(Me_2dazdt)Br_2]$^+$ cation is shown in Fig. 2 and selected bond lengths and angles are reported in Table 2. The metal is essentially within a square planar geometry [max. dev. −0.106(4) Å for S(2)], the ligand is *S*,*S* chelating through the S(1) and S(2) sulfur atoms and two bromide ligands, in a *cis* relationship to complete the geometry around the metal. The coordinated

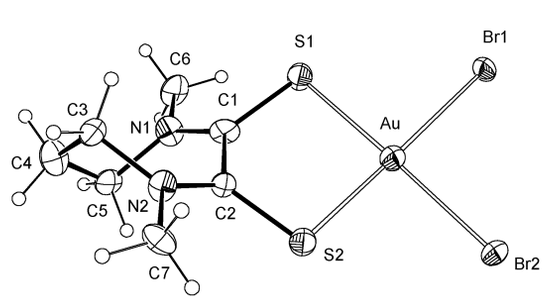

Fig. 2 Molecular structure of the [Au(Me_2dazdt)Br_2]$^+$ cation. The IBr_2^- anion has been omitted for clarity. Thermal ellipsoids are drawn at the 30% probability level.

Table 2 Selected bond lengths (Å) and angles (°) for [Au(Me_2dazdt)-Br_2]IBr_2

C(1)–N(1)	1.32(2)	C(7)–N(2)	1.47(1)
C(1)–C(2)	1.53(2)	C(6)–N(1)	1.45(1)
C(1)–S(1)	1.70(1)	S(1)–Au	2.325(4)
C(2)–N(2)	1.29(1)	S(2)–Au	2.322(4)
C(2)–S(2)	1.68(1)	Br(2)–Au	2.468(2)
C(5)–N(1)	1.48(2)	Br(1)–Au	2.501(2)
C(5)–C(4)	1.52(2)	Br(4)–I(1)	2.742(3)
C(4)–C(3)	1.51(2)	Br(3)–I(1)	2.682(2)
C(3)–N(2)	1.52(2)		
Br(2)–Au–Br(1)	92.39(6)	C(1)–N(1)–C(5)	120(1)
S(1)–Au–Br(1)	88.5(1)	C(6)–N(1)–C(5)	119(1)
S(2)–Au–Br(2)	87.9(1)	C(2)–N(2)–C(7)	120(1)
S(2)–Au–S(1)	91.3(1)	C(2)–N(2)–C(3)	122(1)
C(1)–S(1)–Au	98.5(5)	C(7)–N(2)–C(3)	118(1)
C(2)–S(2)–Au	99.6(5)	Br(3)–I(1)–Br(4)	178.61(7)
C(1)–N(1)–C(6)	120(1)		

ligand adopts a "twist" conformation as found for the Me_2dazdt·IBr adduct with a pseudo two-fold axis passing through the C(4) and gold atoms. The cation complex is chiral but both enantiomers are present in the structure (space group *C*2/*c*). As a consequence of the coordination to the metal, the torsion angle τ[N(1)–C(1)–C(2)–N(2)] [−50(2)°] is sensibly decreased with respect to the corresponding one in Me_2-dazdt·IBr. The C=S bond lengths are longer if compared to the one reported for the uncoordinated C(1)=S(1) group of Me_2dazdt·IBr but comparable to the C(2)=S(2) bond length of this thioxo group involved in the adduct formation (see Tables 1 and 2).

A comparison between [Au(Me_2dazdt)I_2]I_3 [12] and [Au(Me_2-dazdt)Br_2]IBr_2 complexes reveals the presence of significantly shorter S–Au bond distances for the latter complex [2.351(4) and 2.371(3) Å for [Au(Me_2dazdt)I_2]I_3 and 2.325(3) and 2.322(3) Å for [Au(Me_2dazdt)Br_2](IBr_2)] as a result of the greater *trans* influence of the iodide ligand. The thioamide fragments are essentially planar but the twisted conformation of the ligand prevents any electron delocalisation of the two systems. As regards the anion IBr_2^-, the I–Br bond lengths are slightly asymmetric due to a long contact between Br(4) and gold atoms [3.472(2) Å] but the molecule is essentially linear: Br(4)–I(1) 2.742(3), Br(3)–I(1) 2.682(2) Å; Br(3)–I(1)–Br(4) 178.61(7)°. The sum of the two I–Br bond distances (5.4 Å) falls in the range of other structurally characterized IBr_2^- anions.[20] The Raman spectrum in the low frequency region shows a strong peak at 156 cm^{-1} which is assigned to the ν_1 symmetrical stretch of the IBr_2^- unit and two peaks (mw) at 238 and 225 cm^{-1} which are likely to be related to the Au–Br vibrations.[21]

In order to evaluate the effectiveness of IBr- and I_2-adducts in THF solutions compared with the commercial I^-/I_2 aqueous mixtures currently under use for gold dissolution in the etching procedure of microelectronic devices, experiments on gold wires and Si/SiO_2/Ti/Au thin layers (thickness 300 μm/0.5 μm/15 nm/200 nm) have been performed. Wires of the same length and thickness have been dipped into equimolar solutions (c = 5.0×10^{-3} mol dm^{-3}) of the three reagents, then removed, dried and weighed every 10 minutes as shown in Fig. 3, where the gold weight loss ΔW (mg) *vs.* the time (minutes) is reported. Among these reagents the solution of I_2/KI in water reacts very slowly while the Me_2dazdt·$2I_2$ adduct is the most effective in dissolving gold in comparison with the corresponding IBr-adduct. In the case of thin layers, the test specimen has been selected with similar features to those used in microelectronics for photonic devices such as laser diodes.

The etching process has been followed using a metallographic microscope at increasing times (every 50 s) and the overall effect, shown in Figs. 4 and 5 for the Me_2dazdt·2IBr and Me_2dazdt·$2I_2$ adducts, is a fast (only 4 minutes to remove a 200 nm thick gold layer for the diiodine-adduct) and effective

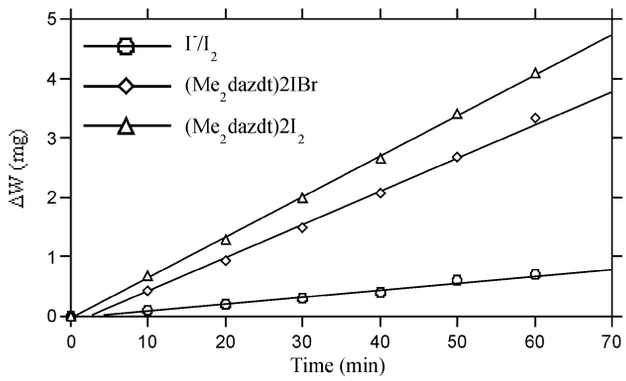

Fig. 3 Plot of the gold weight loss ΔW (mg) *vs.* the time (minutes) for wires of the same length and thickness dipped into equimolar solutions (c = 5.0×10^{-3} mol dm^{-3}) of Me_2dazdt·2IBr and Me_2dazdt·$2I_2$ adducts in THF and I_2/KI in water.

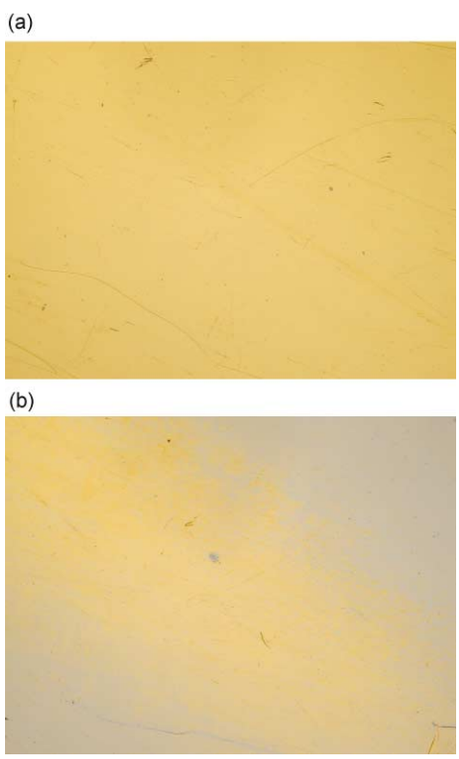

Fig. 4 Gold removal from a Au/Ti (200 nm/15 nm thick) thin layer using a THF solution of the Me_2dazdt·2IBr adduct (c = 5.0×10^{-3} mol dm^{-3}) at t = 0 (a), and 250 s (b).

gold dissolution. The SEM top-view of a detail of Fig. 4(a) is reported in Fig. 6(a) showing that the gold surface, apart from the dark round area which is due to inhomogeneous gold deposition, consists of uniform microtextures. In Fig. 6(b) the SEM top-view of the corresponding etched thin layer [Fig. 4(b)] is reported; it can be observed that the gold etching is uniform (see the evenly etched microtextures) and occurs along preferential lattice crystallographic axes (see the polygonal shape of the dark areas).

The etching with the currently used I_2/I^- aqueous solution is shown in Fig. 7 where details of a thin layer etched for 5 minutes (a) and for 3 minutes (b) using Me_2dazdt·$2I_2$ are reported. The I_2/I^- etch is slower with respect to the adduct-etching and operates unevenly on the gold metallization, as already observed in the case of the gold removal from aged Ga-As-based devices. The I_2/I^--etched gold surface [Fig. 7(a)] appears porous and its colour changes to red (this colour can be related to colloidal gold nanoparticles).[22] Also the adduct-etching was effective independent of the gold crystalline state. This is very peculiar and makes these reagents suitable for gold removal in aged

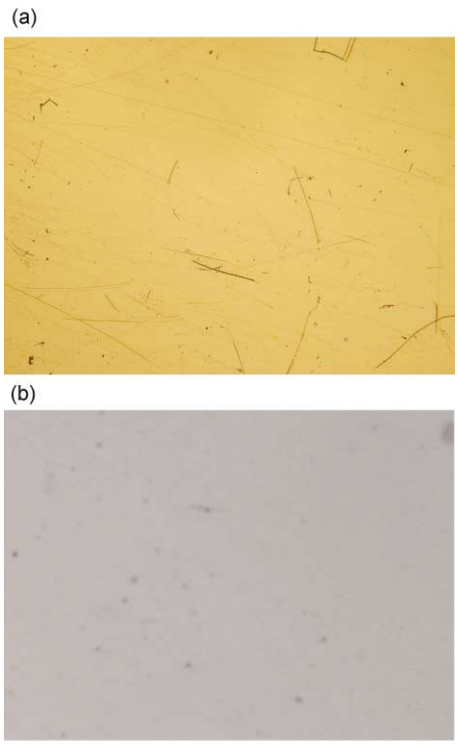

Fig. 5 Gold removal from a Au/Ti (200 nm/15 nm thick) thin layer using a THF solution of the $Me_2dazdt{\cdot}2I_2$ adduct ($c = 5.0 \times 10^{-3}$ mol dm^{-3}) at $t = 0$ (a), and 250 s (b).

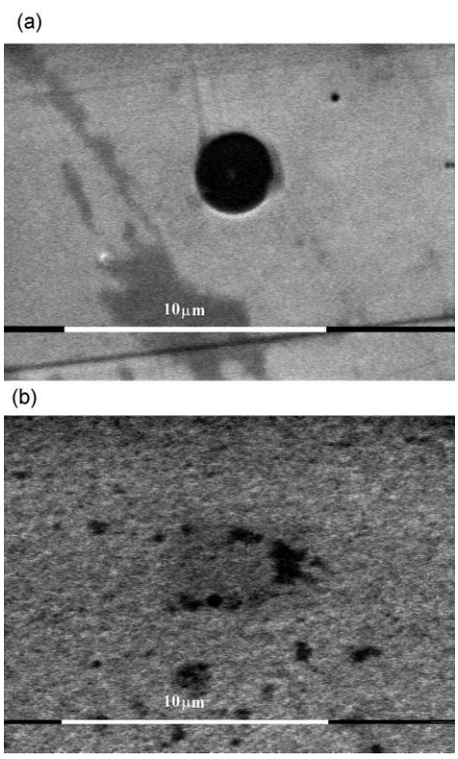

Fig. 6 (a) SEM top-view of the uniform gold surface of a thin layer showing the microtextures; (b) SEM top-view of the gold surface of a thin layer etched for 5 minutes using a $Me_2dazdt{\cdot}2IBr$ adduct in THF solution ($c = 5.0 \times 10^{-3}$ mol dm^{-3}).

devices which show uniform thickness but possibly different local states with respect to crystal structure and contamination.

These results show that these adducts are more effective with respect to the I_2/I^- aqueous mixtures, and between them the diiodine adduct is more powerful. Therefore the electrochemical behaviour of the IBr- and I_2-adducts have been investigated by cyclic voltammetry to check if the redox

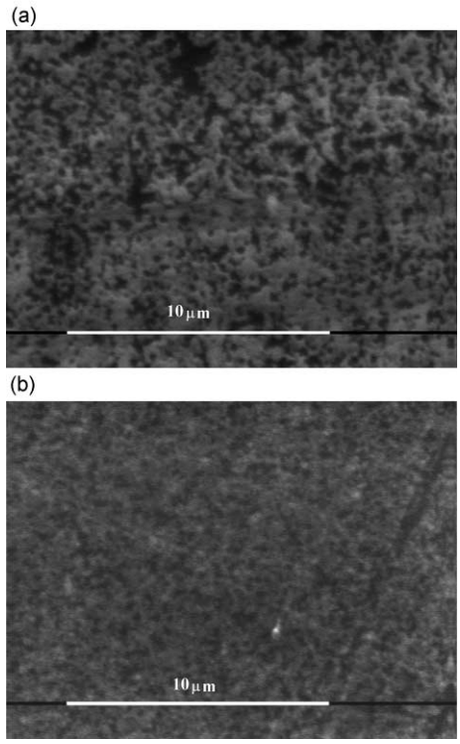

Fig. 7 Comparison between (a) SEM top-view of the gold surface of a thin layer etched for 5 minutes using a I_2/KI aqueous solution ($c = 5.0 \times 10^{-3}$ mol dm^{-3}) and (b) SEM top-view of the gold surface of a thin layer etched for 3 minutes using a THF solution of the $Me_2dazdt{\cdot}2I_2$ adduct at the same concentration.

potential would predict the oxidizing properties of these adducts in gold dissolution. The cyclic voltammograms of $Me_2dazdt{\cdot}2IBr$ and $Me_2dazdt{\cdot}2I_2$ are reported in Fig. 8(a) (anhydrous CH_2Cl_2, scan rate = 0.1 V s^{-1}). Two quasi-reversible reduction waves[23] are observed at $E_{pc}^{1} = 0.536$ V and $E_{pc}^{2} = 0.094$ V for $Me_2dazdt{\cdot}2IBr$ and $E_{pc}^{1} = 0.508$ V and $E_{pc}^{2} = 0.048$ V for $Me_2dazdt{\cdot}2I_2$ when scanning potentials towards the

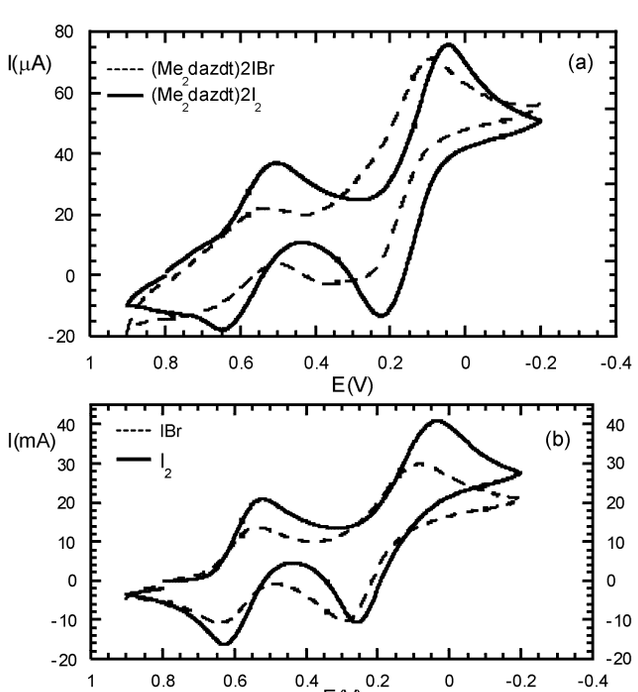

Fig. 8 (a) Cyclic voltammetry (in anhydrous CH_2Cl_2) of the $Me_2dazdt{\cdot}2IBr$ and $Me_2dazdt{\cdot}I_2$ adducts ($c = 1.0 \times 10^{-3}$ mol dm^{-3}). (b) Cyclic voltammetry (in anhydrous CH_2Cl_2) of the free halogens IBr and I_2 ($c = 1.0 \times 10^{-3}$ mol dm^{-3}).

cathodic direction. A comparison with the CVs of IBr (E_{pc}^{1} = 0.534 V and E_{pc}^{2} = 0.084 V) and I_2 (E_{pc}^{1} = 0.524 V and E_{pc}^{2} = 0.042 V) [Fig. 8(b)] suggests that the two reduction waves can be ascribed to the following reduction processes related to the free halogens that appear to be the only electroactive species under the experimental conditions:

$$\tfrac{1}{2}I_2 + e^- \rightleftharpoons I^-$$
$$I^- + X_2 \rightleftharpoons IX_2^-$$
$$IX_2^- + 2e^- \rightleftharpoons I^- + 2X^-$$

where X = I, Br.

These results do not explain the reason why the diiodine adduct is the more effective etching agent. Other effects which are not easily quantified, mainly the stability constants and the solubilities of the formed complexes in the different solvents, should be responsible for the observed effectiveness in the gold etching process of these reagents.

Conclusions

In conclusion, apart the intrinsic interest of the new Me_2dazdt·IBr adduct and the $[Au(Me_2dazdt)Br_2]IBr_2$ complex described here, the relevance of the obtained results relies on the discovery of a class of powerful oxidation reagents which are non-polluting (or at least as environmentally benign as possible), easy to handle and work in a one-step reaction, towards gold. The potential of these reagents has been proved to be high in order to offer to microelectronics technology the possibility of clean, safe and effective etching agents selective for gold dissolution in semiconductor-based laser diodes.

Experimental

Materials

Reagents and solvents of reagent grade purity were used as received from Aldrich. **1** was prepared as already described.[24]

Measurements

Microanalyses were performed on a Carlo Erba CHNS elemental analyzers model EA1108. IR spectra (4000–200 cm^{-1}) were recorded on KBr pellets with a Perkin-Elmer model 983 spectrometer. FT-Raman spectra (resolution 4 cm^{-1}) were recorded on a Bruker RFS100 FT-spectrometer, fitted with an Indium-Gallium-Arsenide detector (room temperature) and operating with an excitation frequency of 1064 nm (Nd:YAG laser). The power level of the laser source varied between 20 and 40 mW. The solid samples were introduced in a capillary tube and then fitted into a compartment designed for a 180° scattering geometry. No sample decomposition was observed during the experiments.

Cyclic voltammograms were obtained using a conventional three-electrode cell consisting of a platinum wire working electrode, a platinum wire as counter-electrode and Ag–AgCl (KCl saturated) as reference electrode. The experiments were performed at room temperature (25 °C), in 1×10^{-3} mol dm^{-3} solutions of the donor containing 0.1 mol dm^{-3} Bu_4NPF_6 as supporting electrolyte, anhydrous CH_2Cl_2 as solvent, at 50–200 mV s^{-1} scan rate. The half-wave potential for the ferrocene/ferrocenium couple (internal standard) is 0.43 V at the above conditions. A stream of argon was passed through the solution prior to the scan. Data were recorded on a EG&G (Princeton Applied Research) potentiostat-galvanostat model 273. The ecthing tests were performed using THF solutions of the Me_2dazdt·2IBr and Me_2dazdt·$2I_2$ adducts having $c = 5.0 \times 10^{-3}$ mol dm^{-3} on wires (0.25 mm diameter, 99.9% Aldrich). The same tests were performed using THF solutions of Me_2dazdt·2IBr and Me_2dazdt·$2I_2$ ($c = 5.0 \times 10^{-3}$ mol dm^{-3}) and aqueous solutions of I_2/KI at the same concentration on 0.4 × 1.8 mm thin layers Au/Ti (200 nm/15 nm thickness). The etching process has been followed by means of the Olympus BX60M Metallographic Microscope equipped with a 50× objective and by SEM (Philips 525M).

Synthesis of Me_2dazdt·2IBr and Me_2dazdt·IBr

Me_2dazdt·2IBr was prepared by allowing a $CHCl_3$ solution of the ligand (0.1 g, 0.531 mmol) and IBr in a 1 : 2 molar ratio to stand at room temperature; after a few days yellow–orange microcrystals were collected (80% yield). Elemental analysis: found (calc. for $C_7H_{12}N_2S_2I_2Br_2$): C, 14.3 (14.0); H, 1.7 (2.0); N, 4.8 (4.7); S, 8.8 (10.6)%. IR (KBr pellet, cm^{-1}): 1530sbr, 1400ms, 1355m, 1335m, 1285ms, 1270ms, 1260ms, 1190w, 1130ms, 1120ms, 1075w, 1025m, 970m, 825s, 750w, 690w, 605m, 595m, 545mw, 525w, 430w, 330mw. Raman (cm^{-1}): 3000m, 2955m, 2926m, 2910ms, 1530ms, 1462w, 1432w, 1399mw, 1352mw, 1281mw, 1257mw, 1186w, 1121w, 875w, 687mw, 600w, 540mw, 285m, 172vs, 120w. After recrystallization from a CH_3CN solution *via* diethyl ether diffusion lustreous yellow–orange crystals of Me_2dazdt·IBr suitable for X-ray studies were obtained. (80% yield). Elemental analysis: found (calc. for $C_7H_{12}N_2S_2IBr$): C, 21.5 (21.3); H, 2.5 (3.0); N, 7.1 (7.1); S, 14.4 (16.3)%. IR (KBr pellet, cm^{-1}): 1535s, 1520s, 1455m, 1445w, 1400ms, 1385ms, 1360w, 1340m, 1290ms, 1280ms, 1260ms, 1220w, 1190w, 1125ms br, 1105ms, 1080mw, 1060w, 1030m, 970m, 830s, 755mw, 685mw, 615ms, 600m, 550w, 520w, 455w, 420w, 340mw. Raman (cm^{-1}): 2919m, 1535ms, 1455mw, 1431w, 1398mw, 1355mw, 1277mw, 1260w, 1217w, 1190w, 1126w, 1061w, 1026vw, 883w, 831w, 685mw, 608w, 596w, 541m, 521w, 409w, 335mw, 252w, 237w, 162s br, 145 sh, 111mw.

Synthesis of $[Au(Me_2dazdt)Br_2]IBr_2$

Me_2dazdt·2IBr (0.1 g, 0.166 mmol) was dissolved in THF (*ca.* 75 mL) and gold metal powder (99.99%, agglomerated, *ca.* 50 to 5 mesh, Acros) was added in a 1 : 2 molar ratio. The red–brown solution turns to dark-brown and after two hours the metal dissolution was complete. The reaction mixture was kept in a diethyl ether diffusion at room temperature. After a week shiny black crystals suitable for X-ray studies were obtained (60% yield). Elemental analysis: found (calc. for $C_7H_{12}N_2S_2AuIBr_4$): C, 9.8 (10.1); H, 0.8 (1.4); N, 3.2 (3.4); S, 6.7 (7.7)%. IR (KBr pellet, cm^{-1}): 2910w, 1563 s,br, 1457mw, 1435w, 1385s, 1327w, 1283w, 1262m, 1113m, 1067w, 1021w, 950w, 822vw, 741w, 600w, 509w, 406w. Raman (cm^{-1}): 2997w, 2952w, 2916mw, 1569m, 1454vw, 1402 mw, 1356 mw, 1282 w, 1109w, 602vw, 530vw, 376m, 354 m, 238m, 225m, 184m, 165sh, 156vs, 129m.

X-Ray crystallography

A summary of data collection and structure refinement are reported in Table 3. Single crystal data were collected with a Bruker AXS Smart 1000 area detector diffractometer (Mo-Kα radiation; λ = 0.71073 Å) for Me_2dazdt·IBr and with a Philips PW 1100 diffractometer (Mo-Kα radiation; λ = 0.71073 Å) for $[Au(Me_2dazdt)Br_2]IBr_2$. Cell constants were obtained from a least-squares refinement of 3530 reflections ($1.86 < 2\theta < 27°$) (Me_2dazdt·IBr) and by a least-squares refinement of the setting angles of 24 randomly distributed and carefully centered reflections ($7.40 < 2\theta < 17.15°$) ($[Au(Me_2dazdt)Br_2]IBr_2$). No crystal decay was observed for either compound. An absorption correction using the program SADABS[25] was applied for Me_2dazdt·IBr and a ψ-scan empirical absorption correction[26] was applied for $[Au(Me_2dazdt)Br_2]IBr_2$ which resulted in transmission factors ranging from 0.584–1.00 and 0.672–1.00, respectively. These structures were solved by direct methods (SIR-97)[27] and refined with full-matrix least-squares (SHELXL-97),[28] using the Wingx software package.[29] Non-hydrogen atoms were

Table 3 Summary of crystallographic data for Me_2dazdt·IBr and $[Au(Me_2dazdt)Br_2]IBr_2$

	Me_2dazdt·IBr	$[Au(Me_2dazdt)Br_2]IBr_2$
Empirical formula	$C_7H_{12}BrIN_2S_2$	$C_7H_{12}AuBr_4IN_2S_2$
Formula weight	395.12	831.81
Colour, habit	Yellow, block	Black, needle
Crystal size/mm	0.25 × 0.15 × 0.12	0.25 × 0.10 × 0.10
Crystal system	Monoclinic	Monoclinic
Space group	$P2_1/n$	$C2/c$
a/Å	12.169(1)	26.523(8)
b/Å	7.836(1)	10.191(6)
c/Å	14.425(1)	14.549(7)
β/°	113.808(2)	111.57(2)
V/Å^3	1258.5(2)	3657(3)
Z	4	8
T/K	293(2)	293(2)
λ/Å (Mo-Kα)	0.71073	0.71073
μ/mm^{-1}	6.014	18.686
No. of reflections/ observed $F > 4\sigma(F)$	8165–1872	3567–1605
$R1$	0.0302	0.0408
$wR2$	0.0586	0.0559

$R1 = \Sigma||F_o| - |F_c||/\Sigma|F_o|$, $wR2 = [\Sigma[w(F_o^2 - F_c^2)^2]/\Sigma[w(F_o^2)^2]]^{1/2}$, $w = 1/[\sigma^2(F_o^2) + (aP)^2 + bP]$, where $P = [\max(F_o^2,0) + 2F_c^2]/3$.

refined anisotropically; hydrogen atoms were placed at their calculated positions. The maximum and minimum peaks on the final difference Fourier maps corresponded to 0.754 and −0.532 e Å^{-3} for Me_2dazdt·IBr and 1.722 and −1.392 e Å^{-3} for $[Au(Me_2dazdt)Br_2]IBr_2$. The programs Parst[30,31] and ORTEP3 for Windows[32] were also used.

CCDC reference numbers 195735 and 195736.

See http://www.rsc.org/suppdata/dt/b2/b210281a/ for crystallographic data in CIF or other electronic format.

Acknowledgements

This research was carried out as part of the project "Chemical Methods for Characterization and Deprocessing of Photonic Devices" supported by MIUR-PRIN 2002 09815_003 and Università di Cagliari. The authors are grateful to Dr Simona Podda, for performing SEM measurements and Prof. M. Vanzi, Dip. DIEE, University of Cagliari, for helpful discussion on the etching experiments on gold thin layers.

References and notes

1 See *Platinum/2001* by A. Cowley and M. Steel, http://www.platinum.matthey.com/publications/index.php.
2 Gold is widely used in packages where it makes intimate contact with the active regions as an upper metallization of a complex multilayer system, typically Ti/Pt/Au in GaAs-based devices. It thus plays the role of the first huge barrier to the examination of devices (*i.e.* after life tests, or during the set up of new processing steps); both the uniform layers and the gold wires hide the visual field to the inspecting instruments [mainly SEM (Scanning Electron Microscopy) and EBIC (Electron Beam Induced Current)] and inhibit the surveying of some bulk phenomena which have high diagnostic relevance for failure analysis. A. Bonfiglio, P. Deplano, R. De Palo, G. Salmini, A. Serpe, E. F. Trogu and M. Vanzi, *Proceedings from ISTFA™ (25th International Symposium for testing and Failure Analysis)*, 14–18th November 1999, Santa Clara, California.
3 See EC website http://europa.eu.int/comm/dgs/environment.
4 R. Schulze, *Ger. Offen. DE. 3401961 Cl. C22B3/00*, 23rd August 1984.
5 S. Ubaldini, P. Fornari, R. Massidda and C. Abbruzzese, *Hydrometallurgy*, 1998, **48**, 113.
6 S. M. Godfrey, N. Ho, C. A. McAuliffe and R. G. Pritchard, *Angew. Chem., Int. Ed. Engl.*, 1996, **35**, 2344.
7 Y. Nakao, *J. Chem. Soc., Chem. Commun.*, 1992, 426; Y. Nakao and K. Sone, *Chem. Commun*, 1996, 897.
8 F. Bigoli, P. Deplano, M. L. Mercuri, M. A. Pellinghelli, A. Sabatini, E. F. Trogu and A. Vacca, *J. Chem. Soc., Dalton Trans.*, 1996, 3583.
9 P. Deplano, J. R. Ferraro, M. L. Mercuri and E. F. Trogu, *Coord. Chem. Rev.*, 1999, **188**, 71.
10 F. Bigoli, P. Deplano, A. Ienco, C. Mealli, M. L. Mercuri, M. A. Pellinghelli, G. Pintus, G. Saba and E. F. Trogu, *Inorg. Chem.*, 1999, **38**, 4626.
11 F. Bigoli, M. C. Cabras, P. Deplano, M. L. Mercuri, M. A. Pellinghelli, A. Serpe and E. F. Trogu, unpublished work.
12 F. Bigoli, P. Deplano, M. L. Mercuri, M. A. Pellinghelli, G. Pintus, A. Serpe and E. F. Trogu, *Chem. Commun.*, 1998, 2351.
13 F. Bigoli, P. Deplano, M. L. Mercuri, M. A. Pellinghelli, G. Pintus, A. Serpe and E. F. Trogu, *J. Am. Chem. Soc.*, 2001, **123**, 1788.
14 M. Vanzi, A. Bonfiglio, P. Salaris, P. Deplano, E. F. Trogu, A. Serpe, G. Salmini and R. De Palo, *Microelectron. Reliab.*, 1999, **39**, 1043.
15 P. Deplano, M. L. Mercuri, L. Pilia, G. Pintus, A. Serpe and E. F. Trogu, unpublished work.
16 L. N. Swink and G. B. Carpenter, *Acta Crystallogr., Sect. B*, 1968, **24**, 429–433.
17 N. Bricklebank, P. J. Skabara, D. E. Hibbs, M. B. Hursthouse and K. M. A. Malik, *J. Chem. Soc., Dalton Trans.*, 1999, 3007; P. D. Boyle, J. Christie, T. Dyer, S. M. Godfrey, I. R. Howson, C. McArthur, B. Omar, R. G. Pritchard and G. Rh. Williams, *J. Chem. Soc., Dalton Trans.*, 2000, 3106; F. Bigoli, P. Deplano, M. L. Mercuri, M. A. Pellinghelli and E. F. Trogu, *Phosphorus, Sulfur, Silicon Relat. Elem.*, 1992, **70**, 175; F. Bigoli, P. Deplano, M. L. Mercuri, M. A. Pellinghelli, A. Sabatini, E. F. Trogu and A. Vacca, *J. Chem. Soc., Dalton Trans.*, 1996, 3583; F. L. Lu, M. Keshavarz, G. Srdanov, R. H. Jacobson and F. Wudl, *J. Org. Chem.*, 1989, **54**, 2165; G. Srdanov and F. Wudl, *Polym. Mater. Sci. Eng.*, 1988, **59**, 1074; D. Atzei, P. Deplano, E. F. Trogu, F. Bigoli, M. A. Pellinghelli, A. Sabatini and A. Vacca, *Can. J. Chem.*, 1989, **67**, 1416; F. Bigoli, P. Deplano, M. L. Mercuri, M. A. Pellinghelli, A. Sabatini, E. F. Trogu and A. Vacca, *Can. J. Chem.*, 1995, **73**, 380.
18 A. J. Blake, F. A. Devillanova, A. Garau, F. Isaia, V. Lippolis, S. Parsons and M. Schroder, *J. Chem. Soc., Dalton Trans.*, 1999, 525; N. Bricklebank, P. J. Skabara, D. E. Hibbs, M. B. Hursthouse and K. M. A. Malik, *J. Chem. Soc., Dalton Trans.*, 1999, 3007; C. Knobler, C. Baker, H. Hope and J. D. McCullough, *Inorg. Chem.*, 1971, **10**, 697; P. J. Skabara, N. Bricklebank, R. Berridge, S. Long, M. E. Light, S. J. Coles and M. B. Hursthouse, *J. Chem. Soc., Dalton Trans.*, 2000, 3235; M. Arca, F. A. Devillanova, A. Garau, F. Isaia, V. Lippolis, G. Verani and F. Demartin, *Z. Anorg. Allg. Chem.*, 1998, **624**, 745; W. I. Cross, S. M. Godfrey, S. L. Jackson, C. A. McAuliffe and R. G. Pritchard, *J. Chem. Soc., Dalton Trans.*, 1999, 2225.
19 K. Nakamoto, in *Infrared and Raman Spectra of Inorganic and Coordination Compounds*, John Wiley & Sons, Inc., New York, 4th edn., 1986, pp. 108, 145.
20 F. Bigoli, P. Deplano, M. L. Mercuri, M. A. Pellinghelli, G. Pintus, E. F. Trogu, G. Zonnedda, H. H. Wang and J. M. Williams, *Inorg. Chim. Acta*, 1998, **273**, 175 and references therein.
21 B. Slootmaekers, E. Manessy-Zoupa, S. P. Perlepes and H. O. Desseyn, *Spectrochim. Acta, Part A*, 1996, **52**, 1255.
22 J. Schmitt, P. Machtle, D. Eck, H. Mohwald and C. A. Helm, *Langmuir*, 1995, **15**, 3256.
23 G. Beggiato, G. Casalbore, G. Marconi and M. Mastragostino, *Monatsh. Chem.*, 1983, **114**, 675; B. Speiser, *Curr. Org. Chem.*, 1999, **3**, 171; A. Walcarius, G. Lefevre, J.-P. Rapin, G. Renaudin and M. Francois, *Electroanalysis*, 2001, **13**, 313.
24 R. Isaksson, T. Liljefors and J. Sandstrom, *J. Chem. Res. (S)*, 1981, 43.
25 Area-Detector Absorption Correction, Siemens Industrial Automation, Inc., Madison, WI, 1996.
26 A. C. T. North, D. C. Phillips and F. S. Mathews, *Acta. Crystallogr., Sect. A*, 1968, **24**, 351–359.
27 A. Altomare, M. C. Burla, M. Camalli, G. L. Cascarano, C. Giacovazzo, A. Guagliardi, A. G. G. Moliterni, G. Polidori and R. Spagna, *J. Appl. Crystallogr.*, 1999, **32**, 115–119.
28 G. M. Sheldrick, SHELX97, Programs for Crystal Structure Analysis (Release 97-2), University of Göttingen, Germany, 1997.
29 L. J. Farrugia, *J. Appl. Crystallogr.*, 1999, **32**, 837–838.
30 M. Nardelli, *Comput. Chem.*, 1983, **7**, 95.
31 M. Nardelli, *J. Appl. Crystallogr.*, 1995, **28**, 659.
32 L. J. Farrugia, *J. Appl. Crystallogr.*, 1997, **30**, 565.